Nanoscale

Accepted Manuscript

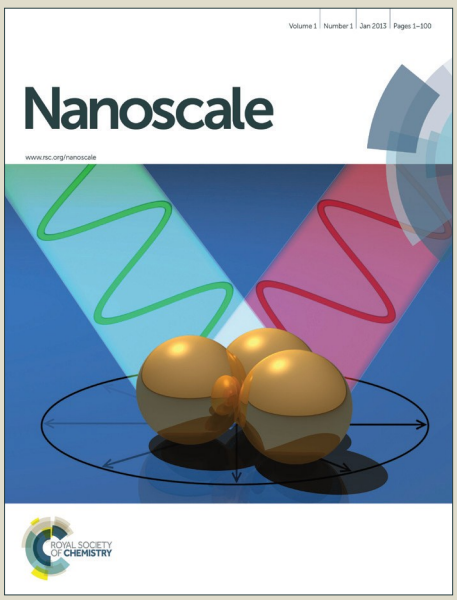

ROYAL SOCIETY OF CHEMISTRY

www.rsc.org/nanoscale

Ascertaining Effects of Nanoscale Polymeric Interfaces on Competitive Protein Adsorption at the Individual Protein Level

*Sheng Song, Tian Xie, Kristina Ravensbergen, and Jong-in Hahm**

Department of Chemistry, Georgetown University, 37th & O Sts. NW., Washington, DC 20057

**Address Correspondence to jh583@georgetown.edu*

ABSTRACT

With the recent development of biomaterials and biodevices with reduced dimensionality, it is critical to comprehend protein adhesion processes to nanoscale solid surfaces, especially those occurring in a competitive adsorption environment. Complex sequences of adhesion events in competitive adsorption involving multicomponent protein systems have been extensively investigated, but our understanding is still limited primarily to macroscopic adhesion onto chemically simple surfaces. We examine the competitive adsorption behavior from a binary protein mixture containing bovine serum albumin and fibrinogen at the single protein level. We subsequently evaluate a series of adsorption and displacement processes occurring on both the macroscopic homopolymer and nanoscopic diblock copolymer surfaces, while systematically varying the protein concentration and incubation time. We identify the similarities and dissimilarities in competitive protein adsorption behavior between the two polymeric surfaces, the former presenting chemical uniformity at macroscale versus the latter exhibiting periodic nanointerfaces of chemically alternating polymeric segments. We then present our novel experimental finding of a large increase in the nanointerface-engaged residence time of the initially bound proteins and further explain the origin of this phenomenon manifested on nanoscale diblock copolymer surfaces. The outcomes of this study may provide timely insight into nanoscale competitive protein adsorption that is much needed in designing bioimplant and tissue engineering materials. In addition, the fundamental understanding gained from this study can be beneficial for the development of highly miniaturized biodevices and biomaterials fabricated by using nanoscale polymeric materials and interfaces.

INTRODUCTION

Protein adsorption to solid surfaces is a widespread phenomenon that crucially impacts a range of applications such as biomedical devices, biosensing, food processing, biofouling, bioreactors and disease diagnostics.[1-3] In particular, these technologically relevant applications typically involve adsorption environments in which multiple protein components simultaneously participate in the surface adhesion. Therefore, under these realistic conditions, it is necessary to consider the competitive and cooperative adsorption of proteins in a multicomponent mixture rather than that of a single type. These multicomponent scenarios present rich and complex adhesion processes that may involve sequential exchanges of surface-bound proteins over time. In this regard, numerous research efforts have been made for the past fifty years in order to understand various competitive surface adsorption processes of different protein mixtures.[1-13]

More recently, understanding single and multi-component protein adsorption behaviors on reduced surface dimensions has also become important with the rapidly increasing demand for miniaturization of biomaterials and biodevices in various *in vivo* and *in vitro* applications.[14-22] Hence, considerable research interests on nanoscale protein adsorption have arisen, focusing on the behavior of individual biomolecules rather than their ensemble characteristics. As a result, unique protein adhesion phenomena, much different than those results from adsorption onto macroscopic scale surfaces, could be revealed at the nanoscale, especially when the physical dimensions of the underlying surface reaches close to the size of an individual protein.[23-29] A suite of experimental techniques including ellipsometry,[19,30] quartz crystal microbalance (QCM),[19,31] surface plasmon resonance (SPR),[32-34] fluorescence-based optical microscopy,[34-36] X-ray photoelectron spectroscopy (XPS),[37,38] and atomic force microscopy (AFM)[20,30,35,39] can be effectively employed for protein adsorption studies in general. However, many cases of the aforementioned nanoscale investigations, requiring a high resolution imaging technique capable of resolving both the nanoscopic details of an underlying surface as well as the subdomain features of individual biomolecules, resorted mainly to AFM.

In particular, nanoscale adsorption behaviors of single component proteins onto polymeric surfaces have been examined previously by us and others by employing the highly surface-sensitive AFM imaging technique and successfully revealing the topographic details present on both the polymeric templates and individual proteins.[23-29,40-42] Interesting protein adsorption phenomena have been elucidated from these research efforts.[14-16] A highly selective behavior was identified from serum albumins (SAs) and other globular proteins on nanoscale diblock copolymer surfaces in which proteins were found to discriminatorily adsorb to preferred polymeric blocks.[23,26] In contrast, more neutral and protein concentration-dependent adsorption behaviors were observed from investigating elongated fibrinogen (Fg) proteins.[29] For this elongated protein, the strongly biased adsorption to a favored polymeric block was seen only at high protein concentrations. However, at low concentrations, both the preferred and non-preferred polymeric blocks played a role in the adsorption process via protein subdomain-specific interactions with different polymer segments. These earlier studies have embarked on a significant step forward in identifying and understanding nanoscale protein adsorption behavior. Yet, our understanding of nanoscale protein adsorption is still far from being complete and, at present, pertains to a single component system. Such knowledge cannot be carried over to effectively predict more complex nanoscale adsorption processes involving different types of proteins.

Valuable insight into multi-component protein adsorption can be gained from hemostasis/thrombosis and biomaterial investigations, although they are in the realm of macroscopic and bulk-scale processes. A vast amount of research has been conducted in the areas of plasma proteins and biomedical implant materials.[1-13,30,37-39] Common protein molecules examined in these studies include plasma protein components such as SAs, immunoglobulins, and Fg.[10] When different proteins are exposed to a solid surface under a competitive adsorption environment, proteins preferentially bound on the surface during early time periods may be displaced by other proteins in the mixture as the competitive adsorption process continues. This general phenomenon of protein exchange in multicomponent protein adsorption is now often referred to as the Vroman effect.[4-9,11-13] From the spearheading research first carried out with dilute blood plasma protein mixtures,[6,11] it is now well-documented that competitive protein

adsorption processes involve a dynamic series of adsorption/desorption and displacement events in which protein species with lower molecular weights, initially arriving at a surface for adsorption to the solid, are later replaced by protein species with higher molecular weights.

Although this general process of Vroman exchange is well known and widely accepted, many aspects of the Vroman effect, including the exact molecular mechanism underlying the process and the precise composition of the adsorbed protein layer from a multicomponent mixture, are still under active investigation. Specifically with regard to nanoscale protein adsorption, it is not known how the competitive adhesion behavior will be manifested on the surfaces of reduced dimensions and to what extent the macroscopic Vroman effect will scale down in nanoscale protein adsorption. Yet, a better understanding of the competitive protein adsorption characteristics at the nanoscale will be beneficial not only in advancing our fundamental knowledge but also in improving biomedical technology. Improved understanding of the competitive adsorption behavior of proteins exhibited at the nanoscale may also result in new thermodynamic and kinetic information as well as the development of nanobiomaterials and nanobiosensors with novel functionalities.

In this study, we undertook the challenge of revealing competitive protein adsorption processes specific to a nanosized surface regime using a model, binary protein mixture. Specifically, we examine the competitive protein adsorption characteristics of a dual-component protein system of bovine serum albumin (BSA) and fibrinogen (Fg) and further elucidate the time- and concentration-dependent protein adsorption profiles on both chemically uniform and alternating polymeric surfaces at the individual protein level. We determine that the time-dependent transition behaviors of surface-bound proteins differ significantly on the polymeric surfaces of polystyrene (PS) homopolymer versus polystyrene-block-polymethylmethacrylate (PS-b-PMMA) diblock copolymer. The two polymeric systems represent adsorption cases in the absence of nanointerfaces for PS, i.e. presenting a chemical uniform surface at the macroscopic level, and in the presence of periodic nanointerfaces for PS-b-PMMA, i.e. presenting chemically alternating domains separated by PS:PMMA interfaces at the nanoscale. The desorption inertia, the extent to which the originally bound protein component resists its displacement

due to other proteins in the bulk phase, is found to be much larger for a nanoscale, chemically alternating surface of PS-b-PMMA when compared to a similar adhesion scenario involving a chemically uniform surface of PS. Specifically, BSA, which preferentially binds to both surfaces at early times, is displaced by Fg much more slowly in the PS-b-PMMA relative to the PS case. This effect is evidenced by a significantly delayed appearance of the turnover window from BSA to Fg on the PS-b-PMMA surface.

This temporally extended, residence time of the initially bound protein species on PS-b-PMMA pertains uniquely to a nanoscale platform whose surface consists of periodically repeating, chemical interfaces on the size scale of individual proteins. We explain the origin of this significant retardation to the onset of a protein exchange process on the surface which is characteristically observed in nanoscale competitive adsorption. Our study marks the first endeavor to illuminate competitive protein adsorption processes specific to a nanoscale size regime, revealing the differences in the competitive protein adsorption processes occurring on polymeric surfaces with and without periodic nanointerfaces on the size scale of individual proteins. Such information will be highly beneficial to the functional design and application of biomaterials and biodevices with reduced dimensionality.

EXPERIMENTAL SECTION

Polymer substrates of PS and PS-b-PMMA were prepared from the homopolymer and diblock copolymer granules received from Polymer Source Inc. (Montreal, Canada). The average molecular weight of PS and PS-b-PMMA (71% PS by weight) is 152 kDa and 71.4 kDa, respectively, with the polydispersity of 1.06. Both chemically uniform (PS homopolymer) and alternating (PS-b-PMMA diblock copolymer) surfaces were made by spin coating 2 % (w/v) polymeric solutions at 3500 rpm for 1 min on Si which was pre-cleaned with a series of solvents using ethanol, acetone, and toluene. Phase separation of PS-b-PMMA was subsequently achieved via thermal annealing in an Ar atmosphere at 240

°C for 6 h with a transient ramp-up rate of 5 °C/min and a cooling rate of 2 °C/min. This process yielded periodically alternating and chemically varying nanodomains known as half-cylinders and exposed repeating stripes of PS and PMMA blocks at the air/polymer interface with repeat units of 45 nm (PS to PS distance).[43,44] BSA and human plasma Fg were purchased from VWR Scientific Inc. (West Chester, PA). The lyophilized powders of BSA and Fg were reconstituted in PBS buffer (10 mM mixture of Na_2HPO_4 and NaH_2PO_4, 140 mM NaCl, 3 mM KCl, pH 7.4) and diluted to varying concentrations ranging from 0.025 to 5 μg/ml. A series of binary protein solutions was made by aliquoting and mixing BSA and Fg solution of desired concentrations. The concentrations of BSA/Fg presented in this study are 5/0.5 μg/mL, 2.5/0.25 μg/mL, 1/0.1 μg/mL, 0.5/0.05 μg/mL and 0.25/0.025 μg/mL. The concentration ratio between BSA and Fg in the bulk solution was kept as 10:1 throughout our competitive adsorption study in order to mimic the typical range of the concentration ratio of the two proteins found in plasma. A volume of 10 μL of the binary protein solution was then delivered to the polymeric substrates and subsequently placed in a humidity-controlled chamber and left for incubation for periods ranging from 5 sec to 48 h. After the incubation period, the sample surfaces were carefully rinsed with 120 μL PBS multiple times, followed by a gentle drying under a stream of N_2 before AFM imaging. Both the individual BSA and Fg proteins as well as the nanoscopic details of the underlying polymeric templates were profiled by performing high-resolution AFM imaging. Subsequently, time-lapse images for a given mixture of concentrations were acquired by imaging multiple, identically treated, samples with varying incubation times. For the AFM images, the topography and phase scans were performed with a MultiMode 8 AFM interfaced with a Nanoscope V controller (Bruker Corp., Santa Barbara, CA), operating in a soft tapping mode at a scan speed of 1 Hz or lower using silicon tips with a typical resonant frequency of 60-70 kHz and a spring constant of 1-5 N/m.

RESULTS AND DISCUSSION

Physical and chemical characteristics of the proteins and polymeric surfaces. SA is a heart-shaped protein with a molecular weight of approximately 66 kDa and is negatively charged at a physiologically relevant pH (pI = 4.8).[10,45-47] SA is comprised of three structurally similar helical domains of I, II, and III, and each domain can be divided into two subdomains of A and B.[48] The physical dimensions of SA are roughly 1.9 nm x 14 nm in height and diameter, respectively, as shown in Fig. 1. Fg is a highly elongated protein also exhibiting negative charges (pI = 5.2) in a physiological environment and is composed of three interwoven polypeptide chains of Aα, Bβ and γ that are connected together by 29 disulfide bonds.[9,10,49] The structure of the 340 kDa dimeric protein consists of rod-like chains spanning roughly spherical domains of D (at the two ends) and E (at the center). The height and length (spanning D-E-D domains) of Fg are approximately 2.3 nm x 55.5 nm, respectively, as shown in Fig. 1. The physical and chemical characteristics of SA and Fg proteins are summarized in Table 1.

Protein	Molecular weight	Diffusion coefficient	Isoelectric point	Number of amino acid residues	Crystal cell dimension[a)]	Physical size[b)]	Concen-tration in Plasma
SA (PDB No: 1E7I)	66 kDa	6.1 x 10^{-7} cm^2/s	4.8	~ 580	a, b, c = 215.7, 45.1, 142.4 Å	1.9 nm x 14 nm	~ 40 mg/ml ~ 600 μmol
Fg (PDB No: 3GHG)	340 kDa	2 x 10^{-7} cm^2/s	5.2	~ 2880	a, b, c = 135.24, 94.87, 300.81 Å	2.3 nm x 55.5 nm	~ 2.5 mg/ml ~ 7.5 μmol

Table 1. Key physical and chemical parameters of SA and Fg are charted. a) The values are taken from the protein data bank (PDB, www.rcsb.org) entry corresponding to the specified PDB number for SA and Fg. b) The physical size was determined by our AFM measurements from the proteins adsorbed on PS.

BSA and Fg were chosen as the two model components in our binary protein adsorption study based on the wealth of knowledge on their bulk-scale and ensemble-averaged adsorption onto solid surfaces.[21,23,29-31,33-36,50,51] In addition, the large shape difference between BSA and Fg makes the identification of the two protein components straightforward via topographical inspection with AFM. A significant body of previous research in the area of biomaterials has provided insight on the adhesion phenomenon of BSA and Fg. Using techniques such as infrared spectroscopy,[21,31] fluorescence-based techniques,[35,36,50,51] SPR,[33,34] QCM,[19,31] XPS,[38] and AFM,[23,29,30,42] the collective adsorption characteristics of single component proteins as well as those of multicomponent protein mixtures have been examined for time-dependent surface adhesion profiles and orientational changes of the surface-bound proteins. In particular, BSA and Fg adhesion onto polymers have been probed on biomedically relevant substrates such as PS, PMMA, polyethylene (PE), polyethylene glycol (PEG), polyethylene oxide (PEO), and polydimethylsiloxane (PDMS),[42,52-57] although the majority of these previous studies pertained to chemically uniform, macroscopic scale, polymeric surfaces. Regardless of the number of protein components in the system under investigation, these prior studies have also concentrated on the collective adsorption characteristics from a large number of proteins, rather than resolving the sequence of adsorption events at the individual protein level. Different from the majority of the aforementioned past studies, our work presented in this paper focuses on the examination of individual proteins at relatively low surface coverage up to a monolayer. This condition was stipulated to perform high resolution AFM imaging while faithfully resolving individual BSA and Fg proteins in their surface-bound state as well as the nanoscopic topological variations of the chemically alternating PS-b-PMMA surface.

PS homopolymer and PS-b-PMMA diblock copolymer are used in this study as the control and test surfaces, respectively, for the binary protein adsorption. Both PS and PMMA are widely exploited as biomedical substrates and products,[58] and their biotechnological relevance makes them suitable for our in-depth protein adhesion study. In addition, PS-b-PMMA diblock copolymer provides self-assembling, nanoscale patterns with a repeat spacing on the order of several tens of nanometers.[57,58] The surface

consists of periodic and well-defined nanoscale surface patterns with distinctive PS and PMMA regions.[43,44] Therefore, the PS-b-PMMA diblock copolymer offers a high density of chemical interfaces defined by the PS and PMMA nanodomains on its surface, unlike the PS homopolymer surface where no chemical interfaces are present. With the use of the PS and PS-b-PMMA platforms, similarities and differences in the binary protein adsorption attributes that are correlated with the presence of nanoscopic features and chemical interfaces on the surface can be revealed.

The characteristic topographies of BSA and Fg on polymeric surfaces are shown in their corresponding AFM panels on the left and right in Fig. 1, respectively. Owing to this large difference in shape anisotropy, BSA and Fg can be easily distinguished on the polymeric surfaces by simple visual inspection, especially for low surface coverage regimes, even though both protein species are simultaneously present on the surface.

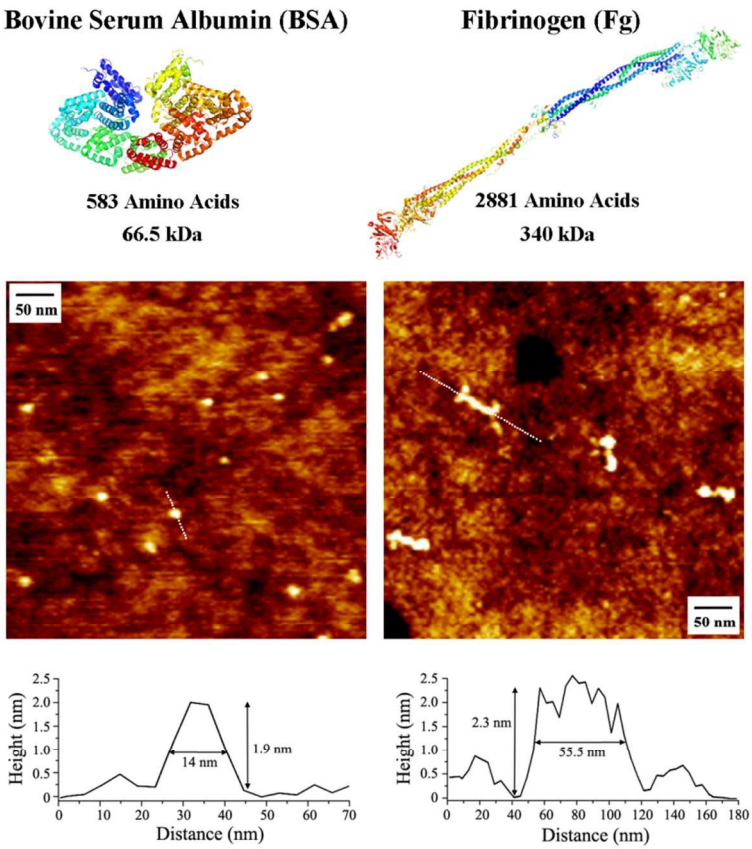

Figure 1. The colored ribbon structures show the two proteins under study, BSA and Fg. The spatial distributions of the amino acid chains of BSA and Fg are depicted to display its heart- and rod-shaped form, respectively. The AFM topography images display the typical sizes and shapes of individually resolved proteins adsorbed on PS foe isotropic BSA (left panel) and highly anisotropic Fg (right panel). Typical line analysis results of the proteins measured along the white lines in the AFM panels are found in the height versus distance profile for BSA (left) and Fg (right).

Various time-lapse phases of the binary protein adsorption. For competitive adsorption of the binary protein mixture on the polymeric surfaces, the two proteins were first combined into a mixture and then delivered onto the control and test platforms. The concentration ratio of the two proteins in the binary mixture was kept constant as BSA:Fg (10:1) in all our experiments, mimicking the typical range of the concentration ratio of the two proteins in plasma. This ratio yields BSA:Fg of approximately 50:1 in terms of the number of protein molecules in the bulk solution. By subsequently conducting time-lapse AFM measurements, we have identified various stages of competitive protein adsorption with increasing interaction time between the proteins and surface. The key stages of the competitive adsorption that are readily identifiable at the individual biomolecular level are the BSA-dominant phase, the Fg onset phase, the Fg turnover phase, and the Fg-dominant phase. In terms of the surface-bound protein counts of BSA and Fg, each of these four phases shows an approximate BSA:Fg ratio of less than 10:1 (BSA dominance), 10:1~5:1 (Fg onset), 5:1~1:10 (Fg turnover), and greater than 1:10 (Fg dominance) in our AFM panels. Fig. 2 illustrates the progressive adsorption frames of the binary protein mixture on the control and test polymeric platforms. On both PS homopolymer and PS-b-PMMA diblock copolymer, the protein component predominantly adsorbed onto the surface initially was identified as BSA, with little to no Fg in view. Examples of this BSA-dominant phase are presented in Fig. 2A(i) for the PS and in Fig. 2B(i) for the PS-b-PMMA case. With increasing incubation time, more and more Fg molecules started to arrive and adhere to the polymeric surfaces, and

both BSA and Fg were easily found on the surface. At this stage, BSA molecules were still abundantly found on the surface, but at least one out of ten protein molecules bound on the surface was revealed as Fg. Such Fg onset phase is displayed in Fig. 2A(ii) and Fig. 2B(ii) for the PS and PS-b-PMMA, respectively. Upon prolonged incubation with the protein mixture, the frequency of Fg molecules continued to increase on the surface, whereas the relative number of BSA was reduced further. In this Fg turnover phase, at least one out of five surface-bound proteins was identified as Fg. The AFM panels corresponding to this stage are found in Fig. 2A(iii) for the PS and Fig. 2B(iii) for the PS-b-PMMA case. With further extended incubation, Fg molecules predominantly occupied the polymeric surfaces. Representative AFM frames of the Fg-dominant phase are displayed in Fig. 2A(iv) for the PS and Fig. 2B(iv) for the PS-b-PMMA platform. The percent surface coverage of the adsorbed proteins in the AFM panels of Fig. 2(A and B) is approximately 3.5% (2A, i), 3.9% (2A, ii), 11.72% (2A, iii), and 47.6% (2A, iv) for the PS case and 2.7% (2B, i), 5.2% (2B, ii), 13.0% (2B, iii), and 39.8% (2B, iv) for the PS-b-PMMA case. As a frame-of-reference, the template morphologies of the two polymeric substrates with no adsorbed proteins can be seen in the AFM images provided in Fig. 2(C).

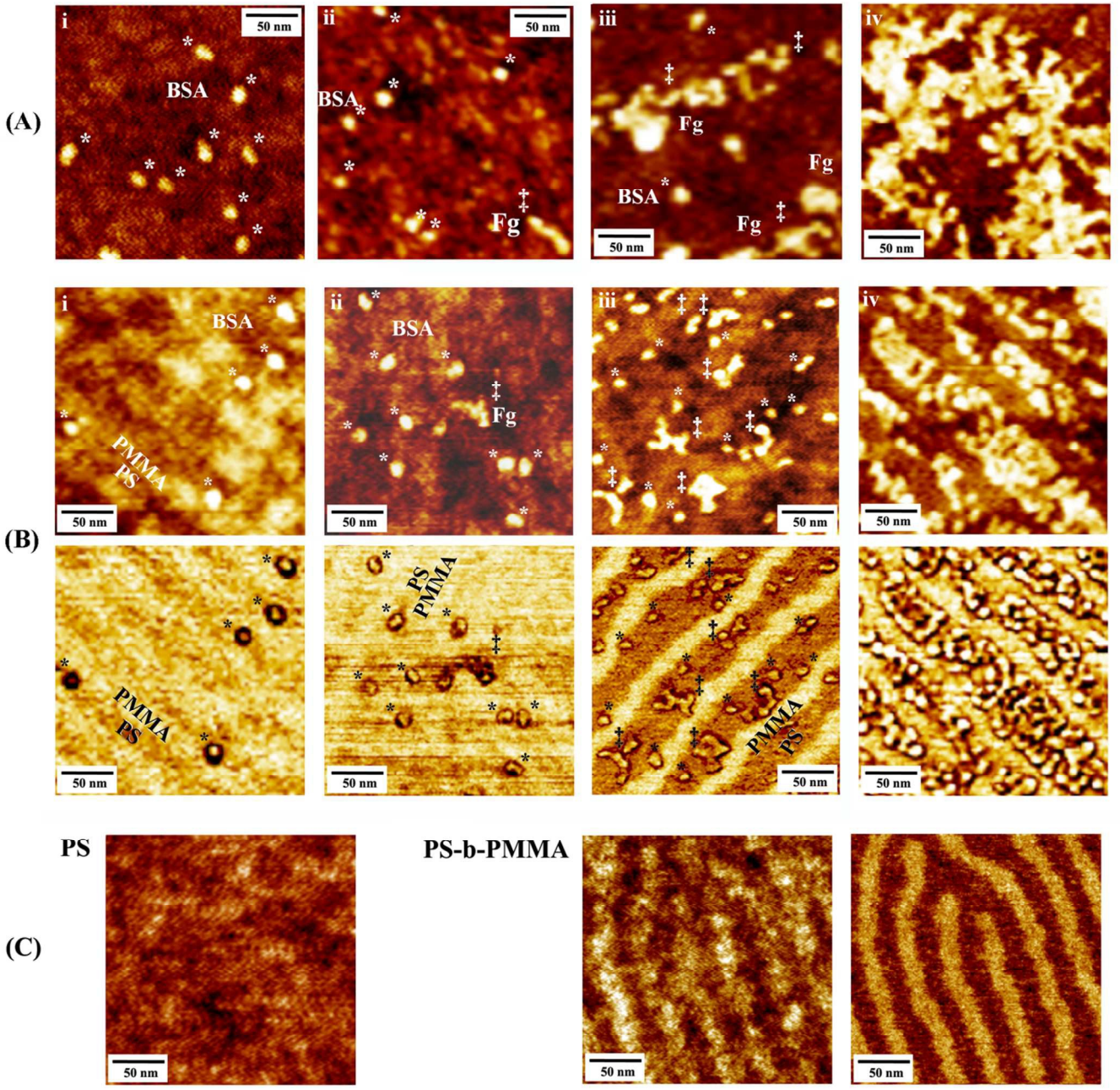

Figure 2. (A) The series of representative AFM panels display the step-by-step views of the four key protein adsorption stages examined by using a mixture of BSA and Fg exposed on the PS homopolymer surface. The protein mixture containing 1 μg/mL BSA and 0.1 μg/mL Fg was incubated on the PS homopolymer surface for 1 min (i), 5 min (ii), 30 min (iii), and 4 h (iv). **(B)** The sequence of AFM images illustrates the progressive snapshots of the competitive protein adsorption evaluated on the PS-b-PMMA diblock copolymer surface. The PS-b-PMMA surface was exposed to the 1 μg/mL BSA and 0.1 μg/mL Fg mixture for 2 h (i), 3 h (ii), 4 h (iii), and 16 h (iv) to allow for competitive protein

adsorption. The AFM images in (A) and (B) illustrate the typical behavior of competitive protein adsorption changing from the BSA-dominant phase (i), to the Fg onset phase (ii), to the Fg turnover phase (iii), and to the Fg-dominant phase (iv). As a guide to the eye for distinguishing the two types of proteins, examples of individual BSA and Fg proteins are marked with * and ‡ in the AFM images, respectively. The phase scans corresponding to each topographic panel in (B) are also displayed in the bottom row in order to present the two protein components as well as the two alternating domains of PS and PMMA underneath the proteins. **(C)** The AFM images of the PS homopolymer (topography panel) and PS-b-PMMA diblock copolymer (left for topography and right for phase panels) surfaces without any bound proteins are displayed.

Instead of the adsorption scenario of the initially bound BSA being displaced by Fg over time, an alternative situation of delayed but increased Fg adsorption may also lead to the progressive transition shown in the time-lapse images of Fig. 2. In this hypothetical situation, Fg adsorption would occur delayed in time onto the surface partially covered by BSA and, without involving any BSA displacement, Fg molecules would predominantly accumulate with higher affinity than BSA on the available surface sites. We carried out an additional AFM and fluorescence tests to examine this possible scenario. We first determined the change in the average numbers of surface bound BSA and Fg molecules over time via direct AFM imaging. For the mixture of 2.5 μg/mL BSA and 0.25 μg/mL Fg deposited for 20 sec on a PS homopolymer, the average number of the PS-bound BSA and Fg was found to be 150±8 and 4±2 protein molecules per 1 μm^2, respectively. After prolonged incubation of 90 min, the surface density of the protein changed to 68±5 for BSA and 75±6 for Fg. This observation clearly indicates that BSA is desorbing from the surface over time under the competitive adsorption environment. We additionally examined the degree of surface-bound BSA at different incubation times by replacing the unlabeled BSA with fluorophore-tagged BSA (ESI, Figure S1†). The resulting fluorescence intensity on the PS-b-PMMA surface showed an increased signal over time under a

noncompetitive adsorption environment involving only the labeled BSA. On the other hand, a slight decrease in intensity was seen under a competitive adsorption involving both the labeled BSA as well as unlabeled Fg. Corroborating the earlier protein density results, this observation also points to the fact that the initially bound BSA is being replaced over time in a simultaneous multi-component adsorption setting. Hence, our experimental data presented in Fig. 2 are progressive snapshots taken from competitive adsorption in which Fg replaces the initially bound BSA with increasing time, rather than depicting the alternative case of delayed Fg adsorption in the environs of permanently bound BSA.

The sequential scenarios presented in Fig. 2 for both the PS and PS-b-PMMA surfaces show that the smaller, more abundant BSA readily adsorbs from the bulk solution onto the polymeric surfaces and, over time, is displaced by the larger, less abundant species of Fg. These outcomes on the PS and PS-b-PMMA surfaces confirm that the Vroman effect is indeed seen not only from the chemically uniform surfaces at the macroscopic scale but also from those surfaces whose chemical compositions alternate at the nanoscale. In our time-dependent protein exchange behavior, the protein species of a lower molecular weight (BSA) is displaced by the higher molecular kind (Fg) over time. The initial adsorption of the more abundant, lighter weight BSA proteins is due to the fact that the mass transfer rate of a solute protein molecule is directly related to the solute concentration and inversely proportional to the solute molecular weight. The faster diffusion of the more concentrated, smaller proteins leads to the initial adsorption on the surface. However, larger proteins are considered to be more surface active as they contain more surface binding domains. Proteins with higher molecular weights can be more flexible in their chain rearrangement and conform to a more energetically favored conformation, which can lead to irreversible adsorption. Therefore, in the Vroman sequence,[4-6,8,9,11-13] the initially adsorbed smaller proteins are expected to be displaced over time by other larger, more strongly interacting proteins. As expected, our results on the macroscopic PS homopolymer surface corroborate the Vroman effect. At the same time, our investigation carried out similarly on the PS-b-PMMA block copolymer surface reveals that this Vroman effect is indeed in effect for the nanoscale competitive protein adsorption case as well.

Time-resolved protein adsorption on PS and PS-b-PMMA with varying concentrations. After carefully examining the different competitive protein adsorption scenarios at different time periods for the macroscopic surface of PS homopolymer (Fig. 3) and comparing to that of the nanoscale PS-b-PMMA case (Fig. 4), we have identified an intriguing effect regarding the time scale associated with the Vroman effect. Fig. 3 displays AFM topographic panels which correspond to the typical view frames of the proteins bound on the PS homopolymer surface at the specified times and BSA/Fg concentrations as annotated in each panel. For the relatively high concentration mixture of 5 μg/mL BSA and 0.5 μg/mL Fg, the PS surface contained quite a few Fg molecules already after 5 sec in addition to BSA. After 1 min, the homopolymer surface was covered with many Fg and comparatively much fewer BSA molecules than before, with Fg making up more than 90% of the surface-bound proteins. The PS surface was covered then entirely with a dense network of Fg after 5 min. For a lower concentration mixture of 1 μg/mL BSA and 0.1 μg/mL Fg, the transition from BSA to Fg occurred more slowly. For this combination, the PS surface was predominantly decorated with BSA even after 1 min and then transitioned to show some individual and small patches of Fg molecules after 5 min. A network of intertwined Fg started to form after 4 h, but the surface coverage of Fg was still below a monolayer. As expected, the surface coverage of the protein molecules was lower with the decreased concentration of the binary mixture when examined after the same duration of incubation time. For the adsorption runs from the mixture of even lower concentrations of 0.25 μg/mL BSA and 0.025 μg/mL Fg, the presence of BSA was still persistent on the PS surface even after 30 min which slowly transitioned after 3h to the stage with both BSA and Fg proteins appearing on the surface. After 16 h, Fg molecules increased in number and tended to assemble close by one another on the PS surface, forming small clusters from several Fg strands. The surface coverage at this concentration was still far from a monolayer even after 16 h.

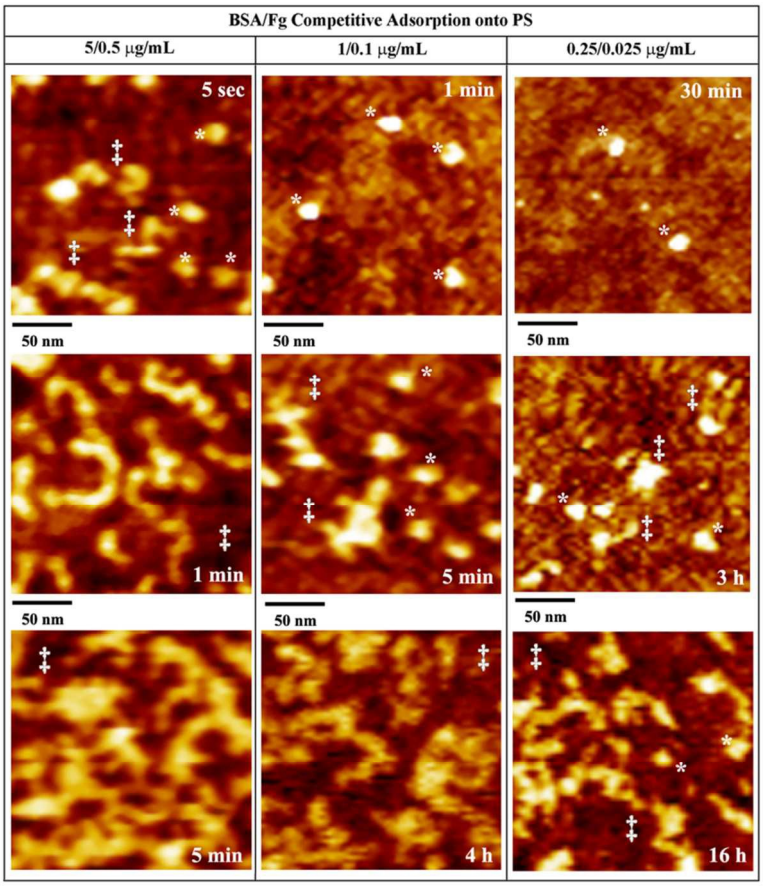

Figure 3. The representative AFM frames capture various time-dependent adsorption stages of the binary protein mixture on the PS homopolymer surface. The images show the progression of the initially BSA-dominant phase (top panels) transitioning to the Fg-dominant phase (bottom panels) observed when using different concentrations of the BSA/Fg protein mixture. As a guide to the eye for distinguishing the two types of proteins, examples of individual BSA and Fg proteins are marked with * and ‡ in the AFM images, respectively.

Similar time-lapse AFM measurements and analyses were subsequently carried out on the nanoscale PS-b-PMMA surface for comparison. The resulting data from the same three sets of BSA/Fg concentrations on the PS-b-PMMA surface are shown in the topographic panels in Fig. 4. At the BSA/Fg concentration of 5 μg/mL and 0.5 μg/mL, the nanoscale surface was still covered largely by BSA after 30 sec. The dominantly appearing BSA molecules were found only on the preferred PS

domain of the PS-b-PMMA due to the greater hydrophobic interaction of the PS domain with BSA. At 5 min, the PS regions were favored by both BSA and Fg, while showing a substantially increased number of Fg molecules and less BSA molecules than before. After 15 min, the PS domains of the PS-b-PMMA surface were filled with more Fg molecules, which then became the dominant species on the surface. For the mixture of 1 μg/mL BSA and 0.1 μg/mL Fg, the BSA-dominant phase was still detected even after 2 h, and the surface slowly turned to increase the Fg footprints after 8 h. However, even at 8 h, the surface was still highly rich with BSA. At 16 h, the PS-b-PMMA surface reached an adsorption state in which a larger fraction of the proteins on the PS domain was identified as Fg. At the even lower mixture concentration of 0.25 μg/mL BSA and 0.025 μg/mL Fg, the BSA to Fg transition on the surface transpired even later than the earlier two concentration sets. Most of the proteins on the PS-b-PMMA surface were BSA at 6 h and 24 h, only increasing the number of BSA proteins found on the surface with longer time. It was only after 48 h that the PS domain on PS-b-PMMA was fully covered largely by Fg. Similar to BSA, Fg adsorption exclusively populated the PS domains of the PS-b-PMMA under our competitive adsorption setting and the PMMA regions were completely free of any protein adsorption.

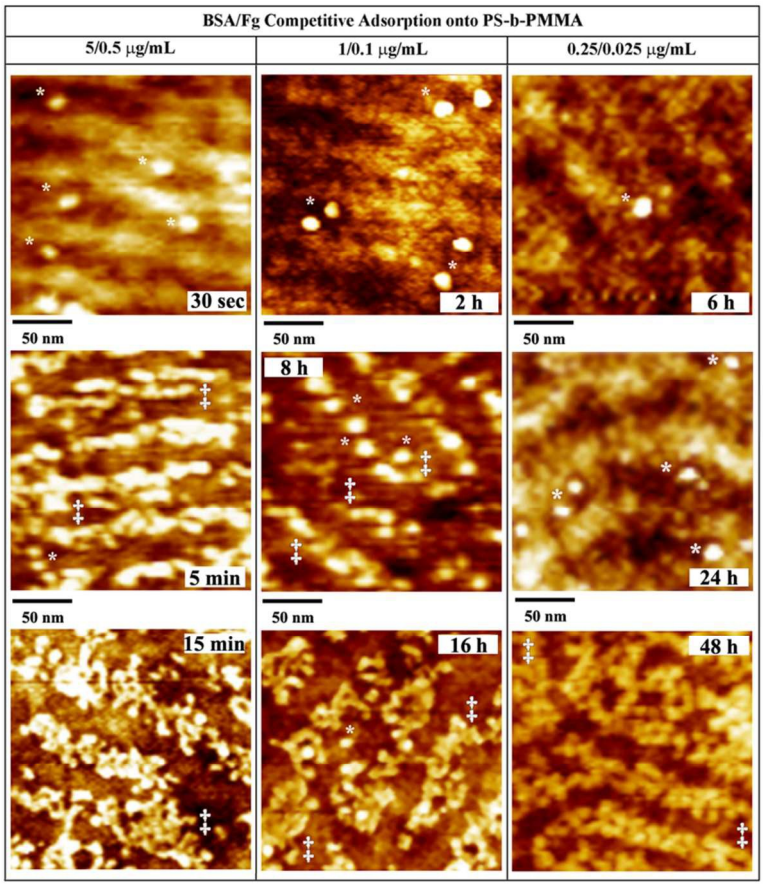

Figure 4. The representative AFM frames display various adsorption stages from the competitive BSA/Fg adsorption onto the PS-b-PMMA surface, profiling the time-lapse views of the initially BSA-dominant phase transitioning to the Fg-dominant phase over time at different concentrations of the BSA/Fg protein mixture. Examples of individual BSA and Fg proteins are indicated with * and ‡ in the AFM images, respectively.

The AFM panels shown in Fig. 5 are the zoomed-out views of each sample examined by utilizing the different polymeric platforms, protein mixture concentrations, and incubation times specified in the images. When further comparing the points in time associated with the displacement of BSA by Fg occurring on the PS homopolymer versus PS-b-PMMA diblock copolymer surfaces, a striking difference was noted from the comparative time-lapse images tracking the two proteins on the two

polymeric surfaces in Fig. 5. In contrast to the competitive adsorption timeline evaluated on the PS surface, our experimental results on the PS-b-PMMA indicate that the time to reach the BSA to Fg turnover state is significantly increased on the PS-b-PMMA surface. This increase in nanointerface-engaged residence time of the initially bound BSA was monitored in all concentration cases of the BSA/Fg mixture when evaluating the competitive protein adsorption scenarios occurring on the PS-b-PMMA platform relative to those on the PS.

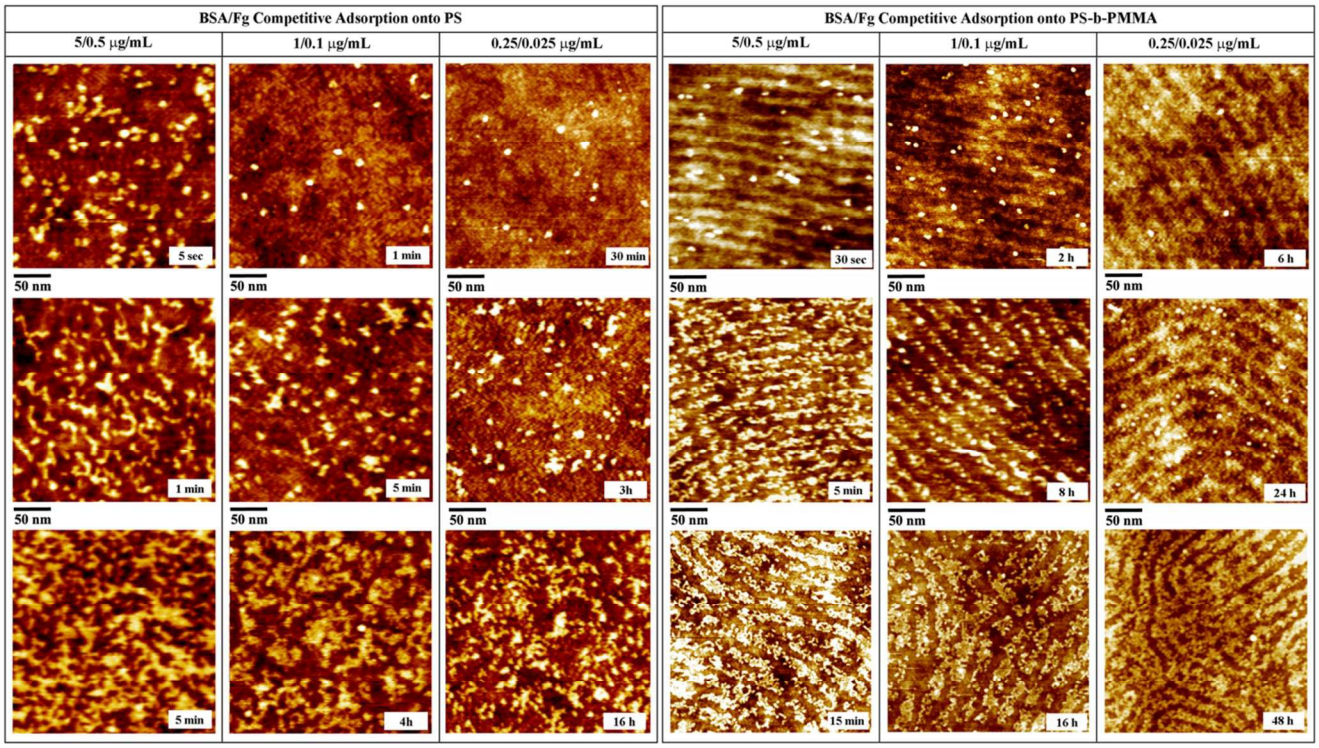

Figure 5. Typical AFM panels of 500 nm x 500 nm in scan size are displayed in order to show larger views of the representative BSA and Fg adsorption behavior corresponding to each polymeric platform, protein mixture concentration, and incubation time specified in the images. Under all scenarios of our competitive protein adsorption experiments, the Fg-rich surface phase occurs after significantly delayed time on the PS-b-PMMA relative to the PS case.

We also assessed Fg adsorption on the two polymeric templates separately under a non-competitive adsorption setting (ESI, Figure S2†). We found that Fg adsorption is more favored on the PS-b-PMMA with the PS:PMMA nanointerfaces relative to the chemically uniform PS surface examined under an identical biodeposition condition. Similar observations of preferred protein binding on diblock copolymer relative to homopolymer surfaces were reported on surfaces with nanoscopic[29,40,41] and macroscopic[59] chemical interfaces. This phenomenon may be explained by the inherent chemical nature of a protein surface where various amino acid residues on the protein exterior are known to exhibit varying degrees of hydrophobicity/philicity and electrostatic charges. Relative to the chemically uniform PS surface, the PS:PMMA interfacial areas of the diblock copolymer can serve as more favorable and stable binding sites towards a greater fraction of amino acids on the protein exterior. Hence, the slower BSA to Fg turnover time observed on the PS-b-PMMA surface in our competitive adsorption study is likely due to the increased BSA residence time on the PS-b-PMMA surface presenting the nanointerfaces, rather than by a potentially reduced affinity in Fg adsorption on the diblock copolymer relative to the homopolymer surface.

Time associated with BSA to Fg transition on PS versus PS-b-PMMA. The unique phenomena observed on the nanoscale diblock copolymer surface relative to the macroscale homopolymer were further ascertained by charting the surface-bound protein composition over time. The resulting time-dependent exchange profiles of surface-bound proteins on the control and test surfaces are presented in Fig. 6. Although only the limited numbers of the representative AFM panels are shown in Figs. 3 through 5, extensive and systematic AFM measurements were additionally carried out on both the PS and PS-b-PMMA surfaces at a substantial number of sampling points under varying adsorption conditions. The concentrations of the BSA/Fg protein mixture tested in our extended competitive adsorption study at the nanoscale were 5/0.5, 2.5/0.25, 1/0.1, 0.5/0.05, and 0.25/0.025 μg/mL for PS-b-PMMA. To compare the results with those on a macroscale surface, the BSA/Fg concentrations of 5/0.5, 1/0.1, and 0.25/0.025 μg/mL were selected for PS. The incubation time of the protein mixture

was varied spanning from 5 sec to 48 h with over 20 different time points used for our time-lapse AFM investigations.

The plots shown in Fig. 6(A) were taken from the competitive adsorption data on the PS-b-PMMA surface by using the five different BSA/Fg mixture concentrations as annotated. As a comparison, the plots shown in Fig. 6(B) are those on PS. The three graphs in Fig. 6(C) illustrate the differences in time spanning the BSA to Fg transition observed from the PS-b-PMMA (chemically alternating at the nanoscale) versus the PS (chemical uniformity persistent at the macroscale) polymers at different protein concentrations, while clearly illustrating the earlier time data. Upon evaluating the large set of concentration- and time-dependent AFM images on both polymeric surfaces, the turnover from BSA to Fg on the PS homopolymer surface was determined to occur even before 5 sec for the BSA/Fg concentration of 5/0.5 μg/mL, between 1-5 min for 1/0.1 μg/mL, and between 30-180 min for 0.25/0.025 μg/mL. On the nanoscale PS-b-PMMA surface, on the other hand, the turnover from BSA to Fg took place between 2-3 min for the BSA/Fg concentration of 5/0.5 μg/mL, 30-45 min for 2.5/0.25 μg/mL, 3-4 h for 1/0.1 μg/mL, 6-8 h for 0.5/0.05 μg/mL, and 24-36 h for 0.25/0.025 μg/mL. The time to reach a Fg-dominant phase with only Fg covering all exposed PS domains of PS-b-PMMA was determined as 15 min, 1 h, 16 h, 24 h, and 48 h for the five sets of BSA/Fg concentrations, respectively.

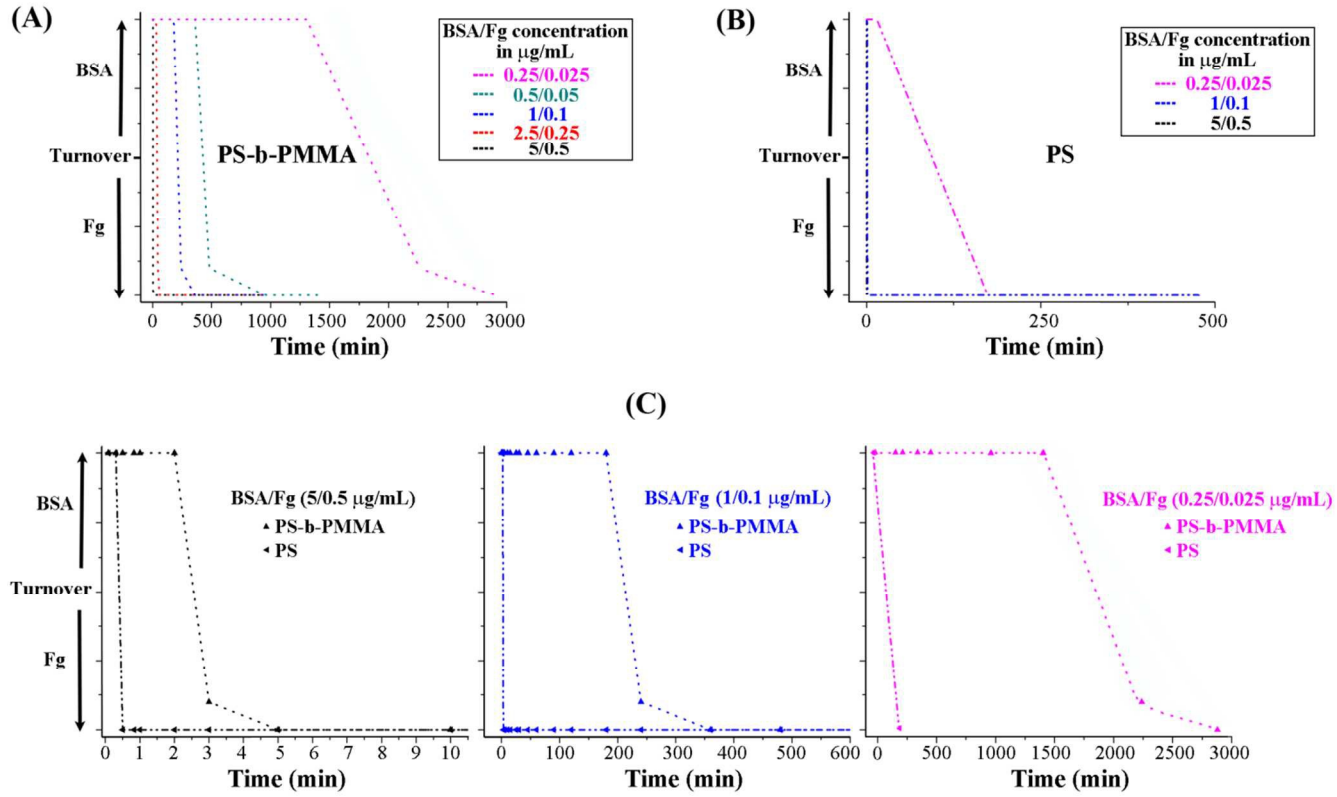

Figure 6. (A) The dominant occurrence profiles of the BSA and Fg proteins adsorbed on the PS-b-PMMA block copolymer surfaces are charted as a function of time at various protein concentrations as indicated in the legend. **(B)** Protein occurrence profiles found on the PS homopolymer surfaces are plotted as a function of time at three different concentrations shown by using the same color-coded plots as (A). **(C)** The three sets of graphs directly compare the time-dependent frequency profiles of the surface-bound protein types found on the PS-b-PMMA diblock and PS homopolymer surfaces for given concentrations. The early time data are shown for easy comparison of the competitive adsorption behaviors on the two different polymeric templates.

The timescale associated with the displacement of the initially adsorbed BSA molecules was determined to be much larger on the nanoscale domains of the PS-b-PMMA diblock copolymer relative to the PS homopolymer, which implies a significant slowdown of the onset of the Vroman effect in

nanoscale competitive adsorption. This effect, confirmed with the extended set of data shown in Fig. 6, is also substantiated in the colored bar graphs shown in Figs. 7(A). The bar graph displays the transitioning stages of the protein type found on the PS-b-PMMA and the PS templates as a function of time. The early time data are clearly seen in the graphs of Fig. 7(B) and can be straightforwardly used to compare between the macroscopic and nanoscale adsorption cases at the three denoted concentrations. The BSA-dominant, BSA/Fg turnover, and Fg-dominant phases are marked in blue, gradient purple, and orange, respectively. The time associated with the transition from BSA to Fg can be revealed by simply identifying the location of the gradient purple block along the vertical axis in these bar graphs. The dependence of protein concentration on the BSA to Fg turnover time is also plotted in Fig. 7(C). The turnover time is inversely proportional to the protein mixture concentration on both the PS-b-PMMA diblock and PS homopolymer surfaces.

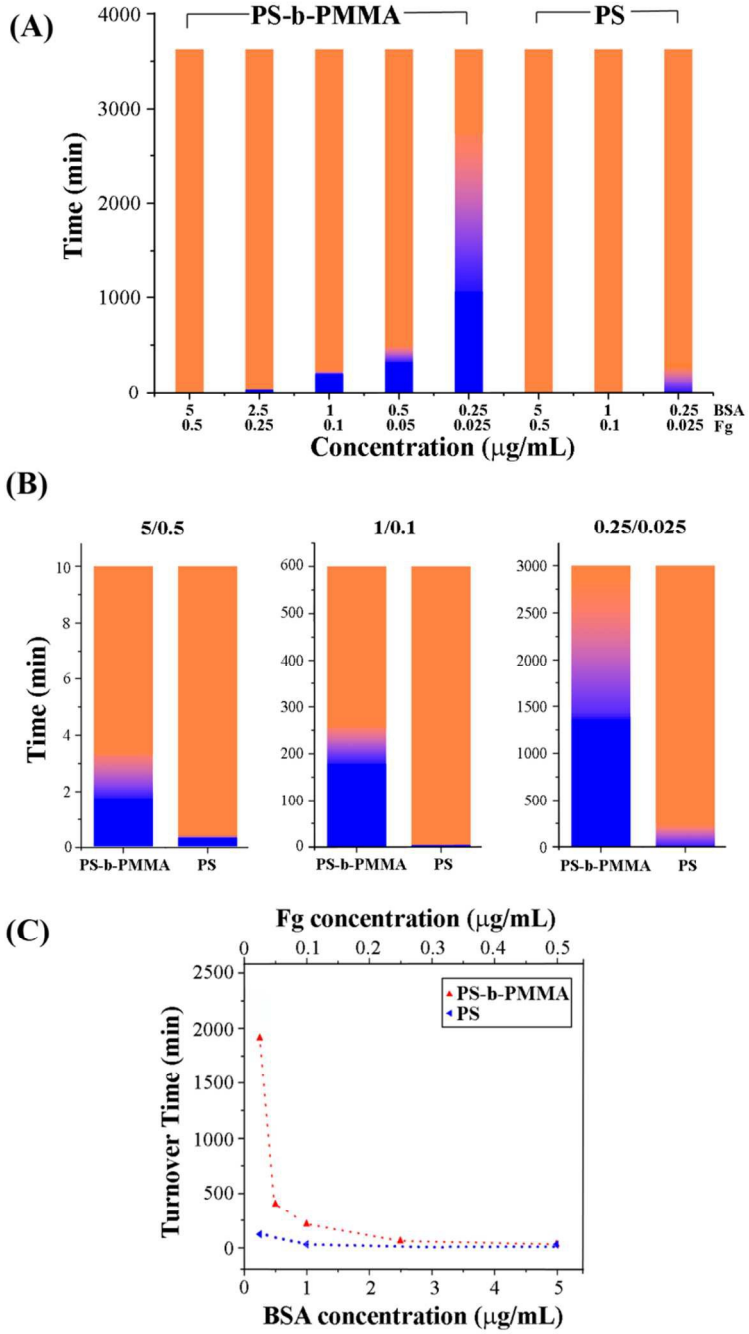

Figure 7. (A) The colored bar graphs display the transitioning stages of the protein type found on the PS-b-PMMA and the PS templates as a function of time. BSA-dominant phase, the Fg onset/turnover phases, and the Fg-dominant phase are identified in blue, gradient purple, and orange, respectively. **(B)** The early stage behaviors of the BSA to Fg transition are captured clearly to display the apparent difference in time marking the Fg turnover phase between the two polymeric templates at the specified protein concentrations. **(C)** The times corresponding to the average turnover point from BSA to Fg are

plotted as a function of the protein concentration. The red and blue data points are taken from the PS-b-PMMA diblock and the PS homopolymer surfaces, respectively.

Understanding the prolonged residence time and the role of nanointerfaces. The large displacement inertia of the originally adsorbed proteins on the PS-b-PMMA relative to the PS surface indicates that the initially bound BSA proteins are more stable on nanosized surfaces, resisting their desorption into the bulk solution over time. This increased stability of the already surface-bound protein molecules and, hence, the prolonged residence time on the nanoscale template may be explained by the more energetically favored surface adsorption environment facilitated by the high density of the PS:PMMA interfaces provided by the repeating blocks of PS and PMMA. Proteins which are highly amphiphilic in surface chemical compositions and properties are known to prefer the surface regions with chemical interfaces, and this effect is best realized when the size scale of the chemical interfaces is commensurate with the size of the individual proteins themselves, i.e. tens of nanometers.[16,25] This interface-preferring adsorption of proteins was previously reported by us and others.[16,23,25,59-61] Proteins in those studies selectively are reported to adsorb on the preferred polymeric domain, e.g. immunoglobulin G (IgG) found only on the PS regions of the PS-b-PMMA and PS/PMMA blend. It has been shown that the protein molecules such as SA, IgG, and fibronectin (Fn) predominantly favor the PS areas closer to the PS:PMMA interface, when their binding affinity within the favored PS domain was further examined with respect to the distance from the interface.[25] In these cases, the PS regions away from the interfaces were left largely unoccupied when the surface coverage of the proteins is low and these initially unoccupied PS areas away from the interfaces become populated by the proteins when loading more proteins to the surface.[23,25,26]

The presence of the densely repeated PS:PMMA chemical interfaces in the PS-b-PMMA support may promote more stable and stronger adhesion of the protein to the underlying surface by satisfying the surface interaction needs of assorted amino acid residues with varying hydrophobicity/philicity present

on the exterior part of the protein molecule. When such needs are met, it will be harder to desorb and displace the protein molecules once they are surface-bound, effectively making the protein inert to other competing desorption or displacement events and leading to the extended residence time of the initially bound proteins. On the other hand, the attachment strength between the same protein molecule to the chemically uniform PS homopolymer will be weaker since the chemically homogeneous environment will limit its favored interactions with relatively smaller number of amino acids and restrict protein conformations on the surface. Therefore, proteins on the PS platform will be more susceptible to desorption incidents into the bulk solution, providing ample opportunities for other proteins to adsorb in its place.

The presence and absence of the chemical interfaces in the PS-b-PMMA versus PS templates, respectively, may also result in two different adsorption scenarios from the electrostatic interaction point of view. On the PS surface, the faster and more abundant BSA molecules will arrive at the surface to a saturation coverage. Further surface adhesion of BSA will be deterred due to the strong repulsion between the adjacent BSA molecules that are negatively charged at pH 7.4. This condition may induce faster BSA desorption events followed by the replacement via Fg whose equilibrium binding constant is six- to seven-fold higher than that of BSA on a hydrophobic surface.[31] On the other hand, such repulsive interactions among BSA molecules may be reduced on the PS-b-PMMA surface since the preferred adsorption domains of PS hosting surface bound BSA molecules are physically separated by the neighboring PMMA domains devoid of any proteins. This environment may yield a longer retention time of the initially bound BSA molecules on the PS-b-PMMA. Further work is underway to ascertain dominant mechanistic pathways associated with the large increase in the nanointerface-engaged residence time of the initially bound proteins.

Although it is known that factors such as increased surface roughness and higher surface area to volume can affect protein adsorption, earlier protein adsorption studies have reported varying outcomes from employing roughened platforms and increased surface areas. For example, the adsorption of SA and Fn on a bioceramic material with an average surface roughness of 32 nm was higher than that with a

142 nm roughness.[62] On the other hand, another study reported that the nanometer-scale roughness variation ranging from 5 to 60 nm did not result in any changes in the adsorbed amount and the structural stability of lysozyme.[63] We note that the phenomenon observed in this study pertains to the PS-b-PMMA surface with an average roughness of 0.32 nm which does not differ greatly from the roughness value of 0.23 nm from the PS surface.[29] When comparing the difference in the substrate roughness to the size of the individual proteins, our polymeric surfaces can be considered to be very smooth adsorption platforms. In addition, both BSA and Fg exhibit a higher binding preference to the PS regions of the PS-b-PMMA. When compared to the PS homopolymer surface with 100% of the exposed surface area being PS, the diblock copolymer presents only about 50% of the exposed surface in the chemical form of PS and consequently offers a much less effective surface area for protein binding. Yet, our competitive adsorption study shows that the binding of the initially bound proteins is much stronger on the PS-b-PMMA surface than that on PS. From these reasons, the effect found in our experiments is believed to have originated from the chemical interfaces repeatedly presented on the nanoscale PS-b-PMMA surface, not from the factors associated with increased surface roughness or specific surface area. Hence, the physical-chemical uniqueness of the PS-b-PMMA diblock copolymer surface, simultaneously providing chemical heterogeneity and reduced dimensionality, is imperative in inducing the prolonged residence time of the initially bound proteins in competitive protein adsorption.

From the fundamental research standpoint, our experimental findings provide deeper insight into competitive protein adsorption behavior that can encompass nanoscale size regimes. We ascertain the similarities and dissimilarities in the time-dependent protein adhesion characteristics that manifest on macroscopic versus nanoscopic polymeric supports. From the biotechnological viewpoint, our work reveals that the use of nanomaterials in biomaterial and biosensor applications, specifically the employment of solid surfaces providing chemical interfaces in the size range of several tens of nanometers, can result in reduced dimensionality- and chemical interface-driven, surface-bound proteins' resistance to desorption by other competing protein molecules in bulk solution. This phenomenon can be utilized in creating protein-stabilizing supports for implant materials and in tissue

engineering, as well as further be exploited to produce antifouling biomedical detection and delivery devices resistant to nonspecific adsorption of undesired proteins.

SUMMARY

In summary, the competitive adsorption characteristics of the model binary protein mixture containing BSA and Fg have been examined on the PS homopolymer and the PS-b-PMMA diblock copolymer by clearly resolving the nanoscale topological details of the individual proteins as well as those of the underlying polymeric templates. The well-known protein exchange process over time was observed from both the macroscopic and nanoscopic polymeric surfaces, in which the initially bound BSA molecules on both the homopolymer and diblock copolymer surfaces were later replaced by Fg. The key stages of the overall turnover processes from the BSA- to Fg-covered phases were identified at various protein concentrations and incubation times by acquiring extensive time-lapse images at the individual protein level from a large set of protein-bound surfaces. The time-dependent protein displacement events on the chemically uniform and alternating polymeric surfaces in the absence and presence of nanoscale chemical interfaces, respectively, were then systematically compared. In contrast to the macroscopic, chemically uniform PS surface, a unique phenomenon was identified on the nanoscale PS-b-PMMA surface pertaining to a large increase in the nanointerface-engaged residence time of the initially bound BSA. The pronounced retardation to the onset of the protein displacement process and the inertia of the originally bound protein in the presence of other competing protein molecules in the bulk solution were explained by the existence of the periodic PS and PMMA chemical interfaces on the size scale equivalent to the individual proteins. The nanospaced chemical interfaces provide more stable and stronger attachment sites for both hydrophobic and hydrophilic binding moieties on the exterior of the protein, rendering the once-adsorbed protein more inert to the competing events of desorption and displacement on the nanoscale template. The insights gained from this study on competitive protein adsorption on nanoscale surfaces, particularly the significant slowdown of the

time-dependent protein exchange process commonly known as Vroman effect, will be valuable in developing biomaterials, biosensors, and biomedical devices with reduced dimensionality functioning in highly miniaturized formats.

ACKNOWLEDGEMENTS

The authors acknowledge financial support on this work by the National Science Foundation (Award No. CHE1404658) from the Macromolecular, Supramolecular and Nanochemistry Program under the Division of Chemistry.

Footnote

†Electronic supplementary information (ESI) available: Fluorescence data on competitive and noncompetitive protein adsorption (Fig. S1) and AFM data of Fg adsorption on PS and PS-b-PMMA in a non-competitive case (Fig. S2).

References

1. K. Nakanishi, T. Sakiyama and K. Imamura, *J. Biosci. Bioeng.*, 2001, **91**, 233-244.
2. M. Rabe, D. Verdes and S. Seeger, *Adv. Colloid Interf. Sci.*, 2011, **162**, 87-106.
3. J. J. Gray, *Curr. Opin. Struct. Biol.*, 2004, **14**, 110-115.
4. L. Vroman, A. L. Adams, G. C. Fischer and P. C. Munoz, *Blood*, 1980, **55**, 156-159.
5. S. M. Slack and T. A. Horbett, in *Proteins at Interfaces II*, Amer. Chem. Soc., 1995, vol. 602, ch. 8, pp. 112-128.
6. L. Vroman and A. L. Adams, *Surf. Sci.*, 1969, **16**, 438-446.
7. W. Norde, F. MacRitchie, G. Nowicka and J. Lyklema, *J. Colloid Interf. Sci.*, 1986, **112**, 447-456.
8. L. Vroman, A. L. Adams, M. Klings and G. Fischer, in *Applied Chemistry at Protein Interfaces*, Am. Chem. Soc., 1975, vol. 145, ch. 12, pp. 255-289.
9. S.-Y. Jung, S.-M. Lim, F. Albertorio, G. Kim, M. C. Gurau, R. D. Yang, M. A. Holden and P. S. Cremer, *J. Am. Chem. Soc.*, 2003, **125**, 12782-12786.
10. J. D. Andrade and V. Hlady, *Annal. New York Acad. Sci.*, 1987, **516**, 158-172.
11. L. Vroman and A. L. Adams, *J. Biomed. Mater. Res.*, 1969, **3**, 43-67.
12. S. L. Hirsh, D. R. McKenzie, N. J. Nosworthy, J. A. Denman, O. U. Sezerman and M. M. M. Bilek, *Colloid. Surf. B: Biointerfaces*, 2013, **103**, 395-404.
13. A. Krishnan, C. A. Siedlecki and E. A. Vogler, *Langmuir*, 2004, **20**, 5071-5078.
14. J. Hahm, *J. Biomed. Nanotech.*, 2011, **7**, 731-742.
15. J. Hahm, *Sensors*, 2011, **11**, 3327-3355.
16. J. Hahm, *Langmuir*, 2014, **30**, 9891-9904.
17. F. A. Denis, P. Hanarp, D. S. Sutherland, J. Gold, C. Mustin, P. G. Rouxhet and Y. F. Dufrêne, *Langmuir*, 2002, **18**, 819-828.
18. M. S. Lord, M. Foss and F. Besenbacher, *Nano Today*, 2010, **5**, 66-78.

19. K. Rechendorff, M. B. Hovgaard, M. Foss, V. P. Zhdanov and F. Besenbacher, *Langmuir*, 2006, **22**, 10885-10888.

20. K. Cai, J. Bossert and K. D. Jandt, *Colloid. Surf. B: Biointerfaces*, 2006, **49**, 136-144.

21. P. Roach, D. Farrar and C. C. Perry, *J. Am. Chem. Soc.*, 2006, **128**, 3939-3945.

22. C. D. Walkey, J. B. Olsen, H. Guo, A. Emili and W. C. W. Chan, *J. Am. Chem. Soc.*, 2012, **134**, 2139-2147.

23. N. Kumar and J. Hahm, *Langmuir*, 2005, **21**, 6652-6655.

24. N. Kumar, O. Parajuli, A. Dorfman, D. Kipp and J. Hahm, *Langmuir*, 2007, **23**, 7416-7422.

25. N. Kumar, O. Parajuli, A. Gupta and J. Hahm, *Langmuir*, 2008, **24**, 2688-2694.

26. N. Kumar, O. Parajuli and J. Hahm, *J. Phys. Chem. B*, 2007, **111**, 4581-4587.

27. O. Parajuli, A. Gupta, N. Kumar and J. Hahm, *J. Phys. Chem. B* 2007, **111**, 14022-14027.

28. S. Song, M. Milchak, H. B. Zhou, T. Lee, M. Hanscom and J. I. Hahm, *Nanotech.*, 2013, **24**, 10.

29. S. Song, K. Ravensbergen, A. Alabanza, D. Soldin and J.-i. Hahm, *ACS Nano*, 2014, **8**, 5257-5269.

30. P. Ying, Y. Yu, G. Jin and Z. Tao, *Colloid. Surf. B: Biointerfaces*, 2003, **32**, 1-10.

31. P. Roach, D. Farrar and C. C. Perry, *J. Am. Chem. Soc.*, 2005, **127**, 8168-8173.

32. R. J. Green, J. Davies, M. C. Davies, C. J. Roberts and S. J. B. Tendler, *Biomaterials*, 1997, **18**, 405-413.

33. J. Breault-Turcot, P. Chaurand and J.-F. Masson, *Anal. Chem.*, 2014, **86**, 9612-9619.

34. Y. Arima and H. Iwata, *J. Mater. Chem.*, 2007, **17**, 4079-4087.

35. A. Toscano and M. M. Santore, *Langmuir*, 2006, **22**, 2588-2597.

36. S. P. Boulos, T. A. Davis, J. A. Yang, S. E. Lohse, A. M. Alkilany, L. A. Holland and C. J. Murphy, *Langmuir*, 2013, **29**, 14984-14996.

37. M. Holmberg, K. Stibius, N. Larsen and X. Hou, *J. Mater. Sci.: Mater. Med.*, 2008, **19**, 2179-2185.

38. R. Michel, S. Pasche, M. Textor and D. G. Castner, *Langmuir*, 2005, **21**, 12327-12332.

39. S. Kidoaki and T. Matsuda, *Langmuir*, 1999, **15**, 7639-7646.

40. K. H. A. Lau, J. Bang, C. J. Hawker, D. H. Kim and W. Knoll, *Biomacromolecules*, 2009, **10**, 1061-1066.

41. K. H. A. Lau, J. Bang, D. H. Kim and W. Knoll, *Adv. Funct. Mater.*, 2008, **18**, 3148-3157.

42. T. F. Keller, J. Schönfelder, J. Reichert, N. Tuccitto, A. Licciardello, G. M. L. Messina, G. Marletta and K. D. Jandt, *ACS Nano*, 2011, **5**, 3120-3131.

43. J. Hahm, W. A. Lopes, H. M. Jaeger and S. J. Sibener, *J. Chem. Phys.*, 1998, **109**, 10111-10114.

44. J. Hahm and S. J. Sibener, *J. Chem. Phys.*, 2001, **114**, 4730-4740.

45. T. Peters, *All About Albumin: Biochemistry, Genetics and Medical applications*, Academic Press, San Diego, USA, 1996.

46. S. Curry, H. Mandelkow, P. Brick and N. Franks, *Nat. Struct. Mol. Biol.*, 1998, **5**, 827-835.

47. D. C. Carter and J. X. Ho, in *Advances in Protein Chemistry*, eds. J. T. E. F. M. R. C.B. Anfinsen and S. E. David, Academic Press, 1994, vol. 45, pp. 153-203.

48. K. A. Majorek, P. J. Porebski, A. Dayal, M. D. Zimmerman, K. Jablonska, A. J. Stewart, M. Chruszcz and W. Minor, *Mol. Immunol.*, 2012, **52**, 174-182.

49. Z. Yang, I. Mochalkin, L. Veerapandian, M. Riley and R. F. Doolittle, *Proc. Nat. Acad. Sci.*, 2000, **97**, 3907-3912.

50. C. F. Wertz and M. M. Santore, *Langmuir*, 1999, **15**, 8884-8894.

51. C. F. Wertz and M. M. Santore, *Langmuir*, 2001, **17**, 3006-3016.

52. Y. L. Cheng, S. A. Darst and C. R. Robertson, *J. Colloid Interf. Sci.*, 1987, **118**, 212-223.

53. Z. Yang, J. A. Galloway and H. Yu, *Langmuir*, 1999, **15**, 8405-8411.

54. M. Herrmann, P. E. Vaudaux, D. Pittet, R. Auckenthaler, P. D. Lew, F. S. Perdreau, G. Peters and F. A. Waldvogel, *J. Infect. Dis.*, 1988, **158**, 693-701.

55. M. Heuberger, T. Drobek and N. D. Spencer, *Biophys. J.*, 2005, **88**, 495-504.

56. X. Chen, M. C. Davies, C. J. Roberts, S. J. B. Tendler, P. M. Williams, J. Davies, A. C. Dawkes and J. C. Edwards, *Langmuir*, 1997, **13**, 4106-4111.

57. I. Szleifer, *Curr. Opin. Solid State Mater. Sci.*, 1997, **2**, 337-344.

58. S. Kumbar, C. Laurencin and M. Deng, *Natural and Synthetic Biomedical Polymers*, Elsevier Science, San Diego, USA, 2014.

59. B. O. Leung, J. Wang, J. L. Brash and A. P. Hitchcock, *Langmuir*, 2009, **25**, 13332-13335.

60. B. O. Leung, A. P. Hitchcock, R. Cornelius, J. L. Brash, A. Scholl and A. Doran, *Biomacromolecules*, 2009, **10**, 1838-1845.

61. Li, A. P. Hitchcock, N. Robar, R. Cornelius, J. L. Brash, A. Scholl and A. Doran, *J. Phys. Chem. B*, 2006, **110**, 16763-16773.

62. E. Dos Santos, M. Farina, G. Soares and K. Anselme, *J. Mater. Sci. Mater. Med.*, 2008, **19**, 2307-2316.

63. M. Han, A. Sethuraman, R. S. Kane and G. Belfort, *Langmuir*, 2003, **19**, 9868-9872.

TOC Graphics

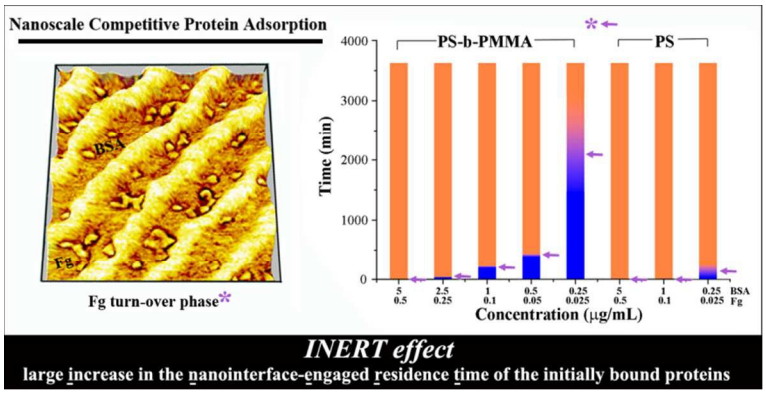

We elucidate nanointerface effects on competitive protein adsorption behaviors at the individual protein level and present findings on protein residence time uniquely observed on nanoscale polymeric surfaces.